Molecular Identification of *Spirometra erinaceieuropaei* Tapeworm in Cases of Human Sparganosis, Hong Kong

Tommy H.C. Tang,[1] Samson S.Y. Wong,[1] Christopher K.C. Lai,[2] Rosana W.S. Poon,[2] Helen S.Y. Chan, Tak Chiu Wu, Yuk-Fai Cheung, Tak-Lap Poon, Yi-Po Tsang, Wai-Lun Tang, Alan K.L. Wu

Human sparganosis is a foodborne zoonosis endemic in Asia. We report a series of 9 histologically confirmed human sparganosis cases in Hong Kong, China. All parasites were retrospectively identified as *Spirometra erinaceieuropaei*. Skin and soft tissue swelling was the most common symptom, followed by central nervous system lesions.

Sparganosis is a parasitic zoonosis endemic in Asia, Europe, and North America. Diphyllobothroid tapeworm under the genus *Spirometra* is the causative agent. Humans can be infected through the consumption of contaminated water or meat from intermediate hosts or through topical application of raw, contaminated poultices to eyes and open wounds. After entry into humans, the plerocercoid larvae (spargana) migrate to different anatomic locations, where they cause space-occupying lesions as they develop into adults. The sites spargana migrate to include skin and soft tissues, muscles, visceral organs, and the central nervous system. Clinical symptoms range from asymptomatic/mild (e.g., subcutaneous swelling) to severe (e.g., seizure and hemiparesis) depending on the site and size of lesions (*1*).

Sparganosis is an emerging zoonotic disease and public health challenge in China, potentially because of the practice of consuming wild frog meat, which is a delicacy in the southern Guangdong province. According to a 2009 survey, >25% of the local wild frogs were infected with spargana (*2*). Most cases of human sparganosis have been found in Asia, with the highest cumulative number in China (online Technical Appendix Table, https://wwwnc.cdc.gov/EID/article/23/4/16-0791-Techapp1.pdf) (*3*). In Hong Kong, the earliest known cases of sparganosis were 2 subcutaneous infections reported in 1962 (*4*), and cases afterward have been sporadic. With advances in molecular sequencing, the identification of sparganum larvae isolated from humans was made possible (*5*,*6*). In this study, we performed molecular sequencing on archived histologic specimens to delineate the parasites down to species level.

Author affiliations: Queen Elizabeth Hospital, Hong Kong, China (T.H.C. Tang, C.K.C. Lai, H.S.Y. Chan, T.C. Wu, Y.-F. Cheung, T.-L. Poon); The University of Hong Kong, Hong Kong (S.S.Y. Wong, R.W.S. Poon); Pamela Youde Nethersole Eastern Hospital, Hong Kong (Y.-P. Tsang, W.-L. Tang, A.K.L. Wu)

DOI: http://dx.doi.org/10.3201/eid2304.160791

The Study

Cases of human sparganosis were identified by searching the clinical, parasitologic, and histopathologic records in the Queen Elizabeth Hospital and the Pamela Youde Nethersole Eastern Hospital in Hong Kong. Archived histopathology specimens showing parasites compatible with plerocercoids were retrieved for further molecular testing. We made 10–15 (depending on the amount of tissue available) 4-μm sections from each paraffin block; the sections were deparaffinized and suspended in sterile, normal saline. Genomic DNA was extracted from formalin-fixed paraffin-embedded tissue by using a DNA minikit (QIAGEN, Hilden, Germany) according to the manufacturer's instructions. The DNA was eluted in 60 μL of elution buffer and used as template for PCR.

Primer sequences used in this study were cox1-F 5′-CGGCTTTTTTTGATCCTTTGGGTGG-3′, cox1-R 5′-GTATCATATGAACAACCTAATTTAC-3′, 28S-F 5′-CACCGAAGC CTGCGGTA-3′, and 28S-R 5′-GAAGGTCGACCTGGTGAA-3′, which targeted specifically to the *cox1* and 28S rRNA genes of *S. erinaceieuropaei* respectively (*7*). The later primers were designed in-house by multiple alignments of different parasite species. The PCR mixture (25 μL) contained DNA, PCR buffer (10 mmol/L Tris-HCl [pH 8.3], 50 mmol/L KCl, 3 mmol/L $MgCl_2$, and 0.01% gelatin), and 200 mmol/L each deoxynucleoside triphosphate (dNTP) and 1.0 U *Taq* polymerase (Applied Biosystems, Foster City, CA, USA). The mixtures were amplified in 60 cycles of 94°C for 1 min, 55°C for 1 min, and 72°C for 1 min with a final extension at 72°C for 10 min in an automated thermal cycler (Applied Biosystems). Standard precautions were taken to avoid PCR contamination, and no false-positive results were observed in negative controls. PCR products were gel purified by using the QIAquick gel extraction kit (QIAGEN). Both strands of the PCR products were sequenced twice with an ABI Prism

[1]These first authors contributed equally to this article.

[2]These authors contributed equally to this article.

3700 DNA analyzer (Applied Biosystems). Sequences of the PCR products were compared with known sequences by BLAST analysis (https://blast.ncbi.nlm.nih.gov).

We constructed a phylogenetic tree using the neighbor-joining method with Kimura's 2-parameter correction with ClustalX 1.83 (http://www.clustal.org). We included in the analysis the 252 bps and 211 bps of the amplicon from the *cox1* gene (GenBank accession nos. KU760072–81) and the 28S rRNA gene (accession nos. KX831668–77) of *S. erinaceieuropaei*, respectively, detected in positive samples. *Strongyloides stercoralis* was used as the outgroup in these analyses.

Seven patients with human sparganosis were identified in Queen Elizabeth Hospital, and 2 patients were identified in the Pamela Youde Nethersole Eastern Hospital. All diagnoses were made from 1999 to 2015 (Table). Eight patients were Chinese; 1 was Filipino, and 4 were male. Patient age at diagnosis was 29–73 (median 49) years. Three patients displayed neurologic symptoms, such as numbness, weakness, or memory impairment, and the other 6 displayed skin and soft tissue involvement. All had progressively enlarging or migratory skin nodules (Table). Additional information on clinical history, histopathology, and magnetic resonance brain imaging of representative cases was collected (online Technical Appendix).

Nine patients had archived histopathologic specimens available for molecular testing. Parasite identification was achieved in all 9 specimens, and they showed 99%–100% and 100% identity with the *cox1* and 28S rRNA gene sequences of *S. erinaceieuropaei*, respectively (Figure, panels A and B).

Conclusions

This study demonstrates that human sparganosis appeared sporadically in Hong Kong. The most common signs of disease were skin and soft tissue nodules followed by intracranial lesions. By molecular sequencing, the tested parasites were *S. erinaceieuropaei.* We were unable to pinpoint the source of infection in most patients; the incubation period can last as long as several months, and early stages of the disease are usually asymptomatic (*8*). Patients might have difficulty recalling specific high-risk exposures. In most industrialized countries, the practice of applying raw frog or snake poultices to open wounds is regarded as unhygienic and becoming obsolete, yet consumption of undercooked frog meat or, less commonly, ingestion of raw snake bile for medicinal purposes is still practiced in Hong Kong. Another possible route of transmission could have been drinking water contaminated with *Spirometra* procercoids.

Subcutaneous sparganosis is the most commonly recognized form of the disease. Because sparganosis is rare, it

Table. Characteristics of cases of human sparganosis, Hong Kong, 1999–2015*

Pt no.	Year	Age, y/sex	Ethnicity	Probable place/mode of infection	Location of lesion	Size of worm or lesion, cm	Clinical features	PEC, $\times 10^9$/L (% total WBC count)
1	1999	67/F	Chinese	Unk/Unk	Right breast	0.15 × 0.1 × 0.7, 0.15 × 0.1 × 0.7, 0.1 × 0.5 × 0.5 (lesions excised)	Right breast mass	NR
2	2000	46/M	Chinese	Unk/Unk	NR	0.15 (worm length)	NR	NR
3	2002	29/F	Chinese	Unk/Unk	Epigastrium of abdominal wall	4 × 2.5 × 2 (lesion excised)	NR	NR
4	2003	63/F	Chinese	Unk/Unk	Left thigh	0.6 (maximum dimension of lesion excised)	Progressive enlarging mass for 2 years	NR
5	2004	44/M	Chinese	Unk/Unk	Right thigh	1.5 × 1.5 (lesion); 0.27 × 0.2 × 0.5 (worm)	Right thigh nodule for 6 months	NR
	2014	55/M		Unk/Unk	Right thigh and suspected left frontal lobe	1.6 × 1.3 × 1.4 (lesion)	Recurrent right thigh nodule; suspicious 2 × 5 × 5 mm T2W/FLAIR hyperintensity with contrast enhancement in left frontal white matter	0.22 (3.7)
6	2005	43/F	Chinese	Unk/Unk	Left breast	0.21 (lesion excised)	Progressive enlarging left breast mass	0.1 (0.7)
7	2011	58/M	Chinese	China/ingestion of frogs and snakes	Left chest wall	3 × 2.5 × 1 (lesion)	Left chest wall mass for 3 years	0.21 (2.5)
8	2013	49/F	Filipino	Unk/Unk	Left parietal lobe	0.17 × 0.12 × 0.23 (lesion)	Right-sided numbness and weakness for 2 days	0.1 (1.1)
9	2015	73/M	Chinese	China/ingestion of frogs	Left thigh	0.5 × 0.5 × 0.1 (lesion excised)	Progressive enlarging left inner thigh mass for 1 year	0.21 (4.2)

*All worms were identified as *Spirometra erinaceieuropaei*. NR, not recorded; PEC, peripheral eosinophil count; Pt, patient; T2W/FLAIR, T2-weighted/fluid attenuation inversion recovery; Unk, unknown; WBC, white blood cell.

is seldom considered during an initial patient assessment, although a migratory nodule might raise the suspicion for a helminthic etiology. Diagnosis of sparganosis needs to be confirmed, normally by studying the excised lesions. Even though serologic tests for sparganosis have been described, these assays are not generally available and their performance requires more evaluation (*9*–*13*). In contrast, the presence of tunnel sign, conglomerated rings, bead-shaped enhancements, or images of parasites of various life stages by computerized tomography or magnetic resonance

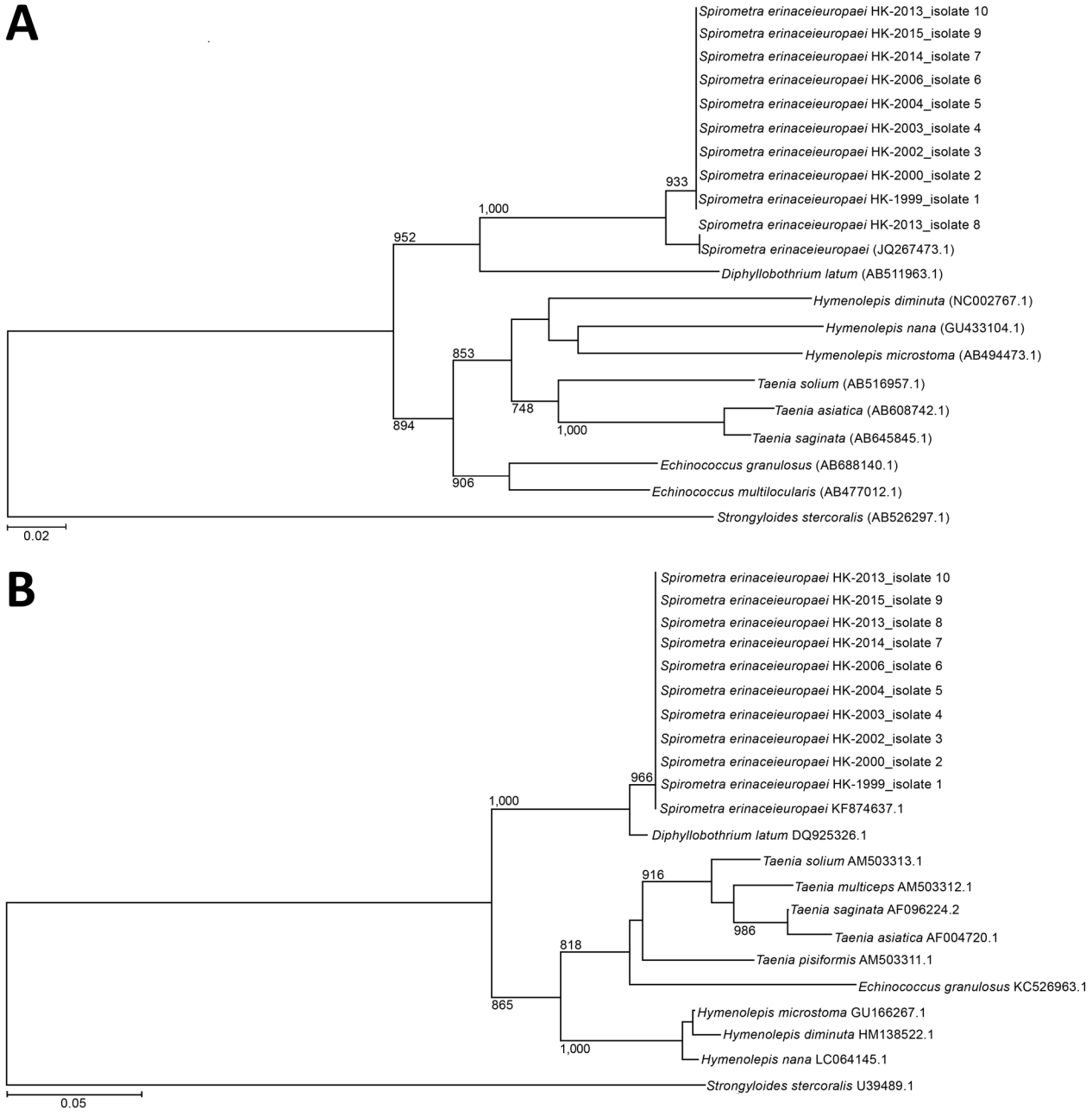

Figure. Phylogenetic analysis of *cox1* and 28S rRNA genes of archived formalin-fixed paraffin-embedded tissues obtained from human sparganosis cases, Hong Kong, 1999–2015. A) A 252-bp sequence from the *cox1* gene (GenBank accession nos. KU760072–81) was included for each isolate. B) A 211-bp sequence from the 28S rRNA gene (accession nos. KX831668–77) was included for each isolate. Trees were constructed by using the neighbor-joining method and rooted with the corresponding sequence in *Strongyloides stercoralis* (accession nos. AB526297.1 and U39489.1 for *cox1* and 28S rRNA genes, respectively). The bootstrap values are shown for nodes that appeared in >70% of the 1,000 replicates. The species used for comparison and their GenBank accession numbers are given in the tree. Scale bars indicate estimated number of substitutions per 50 bases.

imaging are suggestive of sparganosis (*14*). Histopathologic diagnosis of parasitic infections remains a challenge to pathologists in countries where sparganosis is not endemic. Recognizing the different phyla and classes of parasites (i.e., nematodes, cestodes, and trematodes) histologically is usually simple. However, specific identification of the genus and species requires substantial expertise in parasite pathology and morphology. Identification of rare parasites is sometimes impossible because of the lack of detailed morphologic descriptions in the literature. Under such circumstances, molecular studies provide useful information for species identification (*15*). Nevertheless, it is not infallible, especially for rare parasites, because precise species identification depends on gene sequence availability and data accuracy.

Although the parasitic drug praziquantel has wide coverage against several cestodes and trematodes, its efficacy in the treatment of sparganosis remains uncertain. Surgical intervention for complete worm removal should be used whenever feasible.

This study had limitations. We only included information on patients from 2 of the 7 geographic clusters of public hospitals in Hong Kong, and those with asymptomatic subcutaneous lesions most likely did not seek medical attention. The reported number is certainly an underestimate.

Given that human sparganosis is an emerging zoonotic parasitic infection, clinicians may consider it in the differential diagnosis for mass lesions with undetermined etiology. Education of the general public about food safety, including avoiding the consumption of untreated water and undercooked frog and snake meat, is needed.

Acknowledgments

We thank Sherman Lo for providing magnetic resonance imaging brain scans.

Dr. Tang is the associate consultant of the Division of Infectious Diseases in the Department of Medicine at Queen Elizabeth Hospital. His research interests are emerging infectious diseases, infections in immunocompromised hosts, infectious disease epidemiology, and global health.

References

1. Liu Q, Li MW, Wang ZD, Zhao GH, Zhu XQ. Human sparganosis, a neglected food borne zoonosis. Lancet Infect Dis. 2015;15:1226–35. http://dx.doi.org/10.1016/S1473-3099(15)00133-4
2. Li MW, Lin HY, Xie WT, Gao MJ, Huang ZW, Wu JP, et al. Enzootic sparganosis in Guangdong, People's Republic of China. Emerg Infect Dis. 2009;15:1317–8. http://dx.doi.org/10.3201/eid1508.090099
3. Zhang X, Cui J, Liu LN, Jiang P, Wang H, Qi X, et al. Genetic structure analysis of *Spirometra erinaceieuropaei* isolates from central and southern China. PLoS One. 2015;10:e0119295. http://dx.doi.org/10.1371/journal.pone.0119295
4. Huang CT, Kirk R. Human sparganosis in Hong Kong. J Trop Med Hyg. 1962;65:133–8.
5. Boonyasiri A, Cheunsuchon P, Suputtamongkol Y, Yamasaki H, Sanpool O, Maleewong W, et al. Nine human sparganosis cases in Thailand with molecular identification of causative parasite species. Am J Trop Med Hyg. 2014;91:389–93. http://dx.doi.org/10.4269/ajtmh.14-0178
6. Jeon HK, Park H, Lee D, Choe S, Kim KH, Huh S, et al. Human Infections with *Spirometra decipiens* plerocercoids identified by morphologic and genetic analyses in Korea. Korean J Parasitol. 2015;53:299–305. http://dx.doi.org/10.3347/kjp.2015.53.3.299
7. Koonmee S, Intapan PM, Yamasaki H, Sugiyama H, Muto M, Kuramochi T, et al. Molecular identification of a causative parasite species using formalin-fixed paraffin embedded (FFPE) tissues of a complicated human pulmonary sparganosis case without decisive clinical diagnosis. Parasitol Int. 2011;60:460–4. http://dx.doi.org/10.1016/j.parint.2011.07.018
8. Tappe D, Berger L, Haeupler A, Muntau B, Racz P, Harder Y, et al. Case report: molecular diagnosis of subcutaneous *Spirometra erinaceieuropaei* sparganosis in a Japanese immigrant. Am J Trop Med Hyg. 2013;88:198–202. http://dx.doi.org/10.4269/ajtmh.2012.12-0406
9. Yeo IS, Yong TS, Im K. Serodiagnosis of human sparganosis by a monoclonal antibody-based competition ELISA. Yonsei Med J. 1994;35:43–8. http://dx.doi.org/10.3349/ymj.1994.35.1.43
10. Cui J, Li N, Wang ZQ, Jiang P, Lin XM. Serodiagnosis of experimental *Sparganum* infections of mice and human sparganosis by ELISA using ES antigens of *Spirometra mansoni* spargana. Parasitol Res. 2011;108:1551–6. http://dx.doi.org/10.1007/s00436-010-2206-2
11. Rahman SMM, Kim JH, Hong ST, Choi MH. Diagnostic efficacy of a recombinant cysteine protease of *Spirometra erinacei* larvae for serodiagnosis of sparganosis. Korean J Parasitol. 2014;52:41–6. http://dx.doi.org/10.3347/kjp.2014.52.1.41
12. Liu LN, Zhang X, Jiang P, Liu RD, Zhou J, He RZ, et al. Serodiagnosis of sparganosis by ELISA using recombinant cysteine protease of *Spirometra erinaceieuropaei* spargana. Parasitol Res. 2015;114:753–7. http://dx.doi.org/10.1007/s00436-014-4270-5
13. Liu LN, Wang ZQ, Zhang X, Jiang P, Qi X, Liu RD, et al. Characterization of *Spirometra erinaceieuropaei* plerocercoid cysteine protease and potential application for serodiagnosis of sparganosis. PLoS Negl Trop Dis. 2015;9:e0003807. http://dx.doi.org/10.1371/journal.pntd.0003807
14. Lo Presti A, Aguirre DT, De Andrés P, Daoud L, Fortes J, Muñiz J. Cerebral sparganosis: case report and review of the European cases. Acta Neurochir (Wien). 2015;157:1339–43, discussion 1343. http://dx.doi.org/10.1007/s00701-015-2466-9
15. Wong SSY, Fung KSC, Chau S, Poon RWS, Wong SCY, Yuen KY. Molecular diagnosis in clinical parasitology: when and why? Exp Biol Med (Maywood). 2014;239:1443–60. http://dx.doi.org/10.1177/1535370214523880

Address for correspondence: Tommy H.C. Tang, Division of Infectious Diseases, Department of Medicine, Queen Elizabeth Hospital, 30 Gascoigne Rd, Hong Kong, China; email: thc061@gmail.com

Article DOI: http://dx.doi.org/10.3201/eid2304.160791

Molecular Identification of *Spirometra erinaceieuropaei* in Cases of Human Sparganosis, Hong Kong

Technical Appendix

History of Representative Patients

Patient 4

A 63-year-old Chinese woman had a slow-growing mass in her left thigh for 2 years. Physical examination revealed an induration of a 2-cm diameter at the affected area. Microscopic examination of the sections from the excised lesion showed a mixed septal and lobular panniculitis surrounded by palisade of histiocytes and eosinophils. Histologic cross-sections showed viable parasite with folded teguments having brush border, smooth muscles, and calcareous corpuscles inside. No alimentary tract or hooklets could be found. Patient was cured by surgery without recurrence of disease.

Patient 5

A 44-year-old Chinese man had a right thigh nodule for 6 months in 2004. During excisional biopsy, a 1.5 cm × 1.5 cm lipomatous, subcutaneous nodule was removed. Fragments of a worm-like organism of ≈0.5–1 mm in breadth were noted on microscopic examination. The margin of the biopsy was involved. The worm possessed a tegument, beneath which were parenchyma containing additional tegument cells. The parenchyma also contained layers of smooth muscle tissue and calcareous corpuscles. No scolices or hooklets were identified. The subcutis contained a palisade of granulomatous inflammation. On the basis of these morphologic features, a provisional diagnosis of sparganosis was made. Because the margin was involved, a follow-up magnetic resonance imaging (MRI) scan was performed 1 month after surgery. It showed focal skin thickening with mild gadolinium

enhancement subjacent to the surgical scar. Otherwise the images were clear of signs of disease. Another follow-up scan was performed in 2008; this image indicated that the previous gadolinium enhancement that was adjacent to the site of the surgical scar was largely resolved.

In 2014, the patient noted a solitary mass reappearing over the previous surgical site. A small lesion was palpable. MRI showed an ill-defined, contrast-enhancing area of 1.6 cm located over the subcutaneous area of the anteromedial aspect of the right thigh. Microscopic examination of the tissue obtained from a wide excision of the lesion showed multinucleated giant cells surrounding a parasite. An MRI brain scan was performed and showed a 2.0 × 5.0 × 5.0 mm T2-weighted/fluid attenuation inversion recovery hyperintensity with contrast enhancement in the left high frontal white matter. There was no perifocal edema. The lesion remained static on subsequent MRI scan.

Patient 6

A 43-year-old Chinese woman had a nonpainful mass in her left breast. Physical examination showed a 1.5-cm nodule at the 2 o'clock position, 9 cm from the nipple. Ultrasound revealed a hyperechoic area ≈2.1 cm in diameter with ill-defined margins in the left breast. The lesion was subsequently excised; histologic staining of the lesion revealed necrotizing granulomatous inflammation with epithelioid cells, chronic inflammatory cells, and occasional eosinophils. There were no parasites seen in the excised specimen. The patient remained well after surgery without recurrence. Based on patient clinical history and the presence of eosinophils on histology, the clinician sent the tissue for a nucleic acid amplification test.

Patient 7

A 58-year-old Chinese man had a mass in his left chest for 3 years. There was no history of trauma. The mass caused mild pain and pruritus without systemic symptoms. The patient noted some migration of the mass over the years. Further questioning revealed that the patient had a history of frequent travel to mainland China, and he consumed snake and frog meat during these travels. Initial physical examination revealed a firm 1-cm chest wall mass. Results from fine-needle aspiration cytology showed suspected parasitic elements. During excisional biopsy, a 3.0 × 2.5 × 1.0–cm lesion was removed. Postoperative ultrasound showed no residual lesions.

Histopathology showed patchy, suppurative granulomatous inflammation containing a parasite, which contained muscle bands and spherical, dark-staining calcareous corpuscles with whorled appearance scattered in its parenchyma (online Technical Appendix Figure 1, panels A–C). The overall morphology was compatible with sparganosis. Ophthalmologic assessment and computer tomography scans of the brain showed no abnormalities. The patient was well 2 years after surgery with no evidence of disease recurrence.

Patient 8

A 48-year-old Filipino woman reported right-sided weakness and numbness for 2 days. On examination her upper and lower limb power was 4/5 (Medical Research Council scale for muscle power: https://www.mrc.ac.uk/research/facilities-and-resources-for-researchers/mrc-scales/mrc-muscle-scale/). An initial contrast computer tomographic brain scan showed a suspicious ring-like, heterogeneous enhancement at the high-left fronto-parietal region of the brain peripheral to the vertex with an associated perifocal white matter edema at the left corona radiate. The features were highly suspicious of a focal aggressive lesion either at the cortical region or the leptomeningeal region. A contrast MRI brain scan showed 3 enhancing intra-axial lesions in the left cerebral hemisphere (online Technical Appendix Figure 2, panels A–F). The largest one was seen in the high-left parietal, measuring 1.7 × 1.2 × 2.3 cm, and 2 others were noted in high-left parietal and left inferior frontal region with surrounding edema. The radiologic findings were suspected cerebral metastases. Open brain biopsy was performed and showed a thin layer of subdural tissue connected to the left parietal parenchymal lesion, a rubbery parietal lesion having a small amount of whitish discharge inside, and a large cortical vein adhering to the posterior edge of the parietal lesion. Intraoperative frozen-section of the sampled brain tissue showed necrotic and fibrous tissue with infiltrates of lymphocytes, plasma cells, and many eosinophils. Gram, Grocott, periodic acid-Schiff with diastase (PASD), and Ziehl-Neelsen (ZN) stains were negative for microorganisms. Histology of the brain tissue showed necrotic material surrounded by a granulomatous reaction, with chronic inflammatory infiltrates and some eosinophils. There was no evidence of malignancy. A necrotic helminth was identified within the necrotic area. Due to the extensive necrosis, initial identification of the

helminth was deemed impossible. Oral albendazole 400 mg twice daily and dexamethasone 2 mg 4 times daily were given for 2 weeks.

The patient's right-sided numbness persisted. A follow-up MRI brain scan 62 days after the brain biopsy showed that the heterogeneous lesions in the high-left parietal regions were still present and had migrated (online Technical Appendix Figure 2, panels G and H). The scan showed a lesion with a serpentine, elongated configuration and a T2-hypointense signal with hyperintense center together with heterogeneous rim/nodular contrast enhancement. The more anterior lesion appeared larger in size and measured ≈0.8 × 0.8 cm in cross-sections and 1.8 cm in length. It showed deeper involvement into the subcortical white matter. Perifocal T2-hyperintense signal was similar in extent. The posterior lesion was similar in size, measuring 0.1 × 0.6 × 0.2 cm. Perifocal T2-hyperintense signal was more extensive. The left frontal lesion ≈0.7 mm in size showed contrast enhancement with perifocal edema of similar extent. Oral praziquantel 1,500 mg 3 times daily and dexamethasone 2 mg twice daily were given for 1 week after diagnosis of sparganosis was confirmed by molecular sequencing.

The patient had a generalized tonic-clonic seizure 90 days after brain biopsy. The follow-up MRI brain scan 103 days after brain biopsy showed increased caudal extent with deeper involvement into the subcortical white matter for the left frontal lesion. The patient refused to repeat brain surgery for complete excision and received 2 weeks of oral praziquantel 1,500 mg and cimetidine 400 mg 3 times daily. She returned to the Philippines afterwards with residual right-sided limb power of 4+/5.

References

1. Ng TH, Wong WT, Fung CF, Leung CY. Clinical sparganosis in Hong Kong. J R Soc Health. 1989;109:138–40. PubMed http://dx.doi.org/10.1177/146642408910900409

2. Huang CT, Kirk R. Human sparganosis in Hong Kong. J Trop Med Hyg. 1962;65:133–8. PubMed

3. Wong W, Huang C. A case of ocular sparganosis in Hong Kong. Far East Med J. 1970;1:107–9.

4. Chan S-T, Tse CH, Chan YS, Fong D. Sparganosis of the brain. Report of two cases. J Neurosurg. 1987;67:931–4. PubMed http://dx.doi.org/10.3171/jns.1987.67.6.0931

5. Fung CF, Ng TH, Wong WT. Sparganosis of the spinal cord. Case report. J Neurosurg. 1989;71:290–2. PubMed http://dx.doi.org/10.3171/jns.1989.71.2.0290

6. Chuen-Fung TL, Alagaratnam TT. Sparganosis of the breast. Trop Geogr Med. 1991;43:300–2. PubMed

7. Aung TH, Lee MK, Kwok JCK, Leung SCL. How safe is computed tomography-guided stereotaxy in neurosurgery and how should we select patients? Hong Kong Med J. 1995;1:329–34.

8. Kay R; Hong Kong Neurological Society. Casebook of neurology. Philadelphia: Lippincott, Williams & Wilkins; 2002.

9. Chan ABW, Wan SK, Leung S-L, Law BKB, Lai DPY, Ip M, et al. Sparganosis of the breast. Histopathology. 2004;44:510–1. PubMed http://dx.doi.org/10.1111/j.1365-2559.2004.01831.x

Table. Characteristics of previously reported human sparganosis patients*

Patient	Year	Age, y, sex	Ethnicity	Probable place/mode of infection	Location of lesion	Size of worm, L × W, lesion, L, cm	Clinical features	% peripheral eosinophils over total leukocytes	Reference
1	1962	30, F	Chinese	NR/undercooked frog meat	Chest wall	3.0 × 0.1–0.2	Subcutaneous mass	Normal	(*1,2*)
2	1962	2.5, M	NR	Hong Kong/undercooked frog meat	Abdominal wall	NR	Subcutaneous mass	9%	(*1,2*)
3	1970	32, M	Chinese	China/application of raw frog meat	Right eye	8.0 × 1.5–2.0	Migratory subconjunctival swelling	4%	(*1,3*)
4	1987	12, F	Chinese	China/contaminated water	Brain (right frontal)	NR	Convulsion	Normal	(*1,4*)
5	1987	56, M	NR	China/contaminated water	Brain (right parietal)	NR	Progress limb weakness	Normal	(*1,4*)
6	1987	29, M	NR	China/unknown	Right groin	NR	Subcutaneous mass	Normal	(*1*)
7	1988	22, M	Chinese	Macau/unknown	Spinal cord (T9)	4.0 × 0.2	Lower limb weakness and numbness	4%	(*1*)
8	1988	22, M	Chinese	Macau/unknown	Spinal cord (T8–9)	1.0 × 0.5	Low back pain and urinary incontinence	4%	(*5*)
9	1991	47, F	Chinese	Hong Kong/unknown	Right breast	≈4.5	Right breast mass	2%	(*6*)
10	1996	NR, NR	NR	NR/unknown	Brain (parietal lobe)	NR	NR	NR	(*7*)
11	1998	27, F	Chinese	Guangxi province, China/application of raw frog meat poultices	Right basal ganglia	0.22 × 0.15	Left-sided numbness for 36 mo.	Normal	(*8*)
12	2004	80, F	NR	NR/unknown	Left breast	22 × 5	Left breast	NR	(*9*)

*L, length; NR, not recorded; W, width.

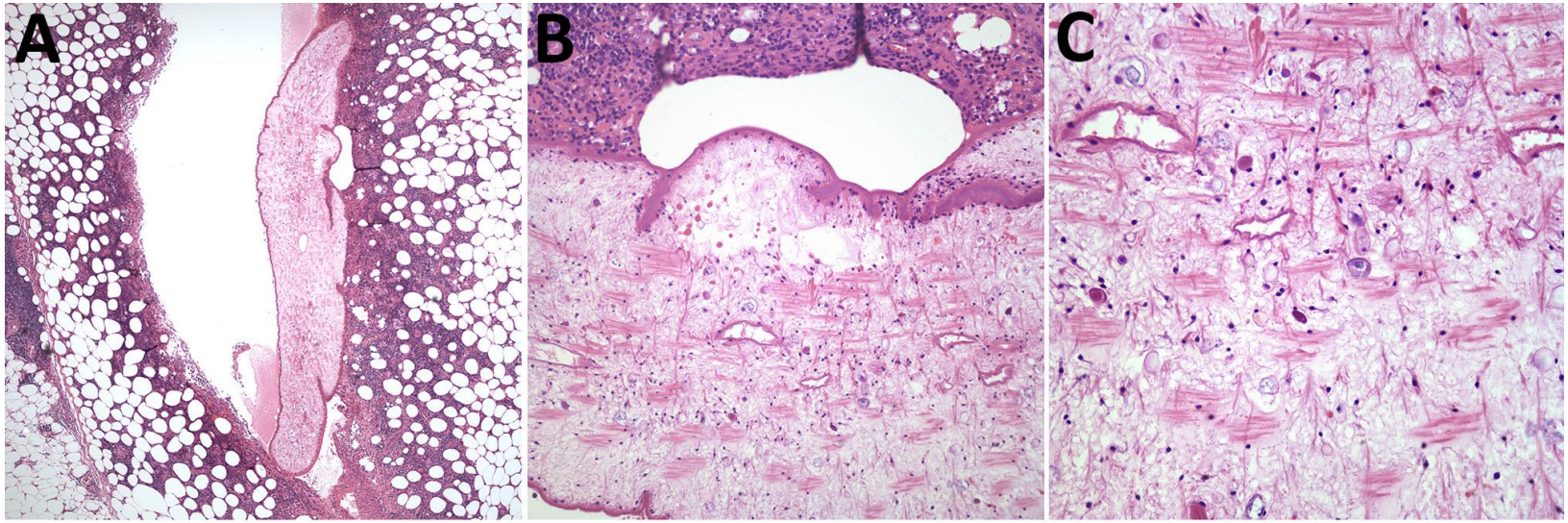

Technical Appendix Figure 1. Hematoxylin-eosin staining of tissue section from lesion in patient 7. A) Scanning view of the lesion (original magnification, 4×). B) Low-power view of the sparganum (original magnification, 20×). C) High-power view of the sparganum (original magnification, 40×).

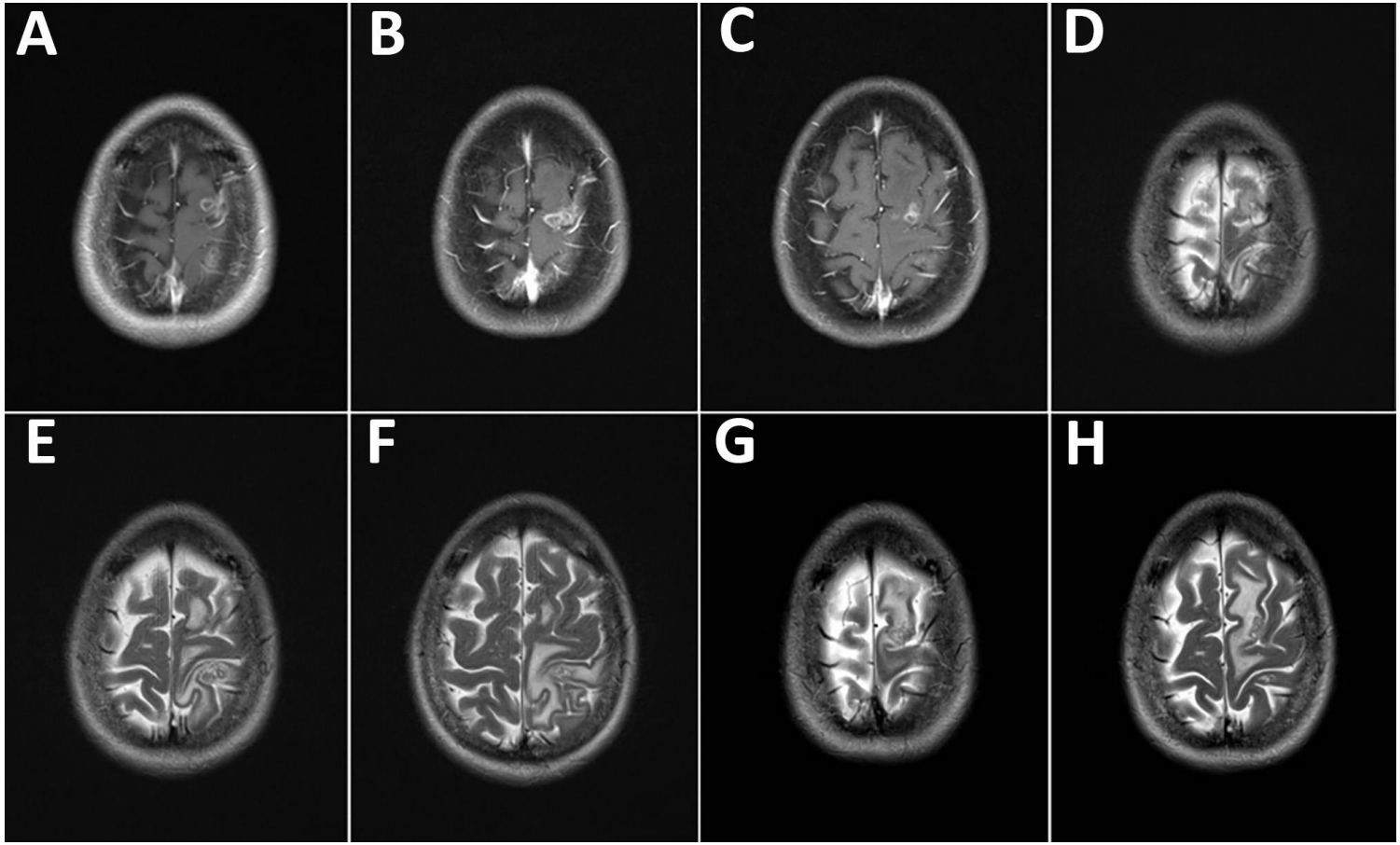

Technical Appendix Figure 2. Serial magnetic resonance imaging (MRIs) brain scans of patient 8. The bottom of the images correspond to the back of the head. A–C) T1-weighted images of initial scan. D–F) T2-weighted images of initial scan showing 3 lesions in the left high parietal and left inferior frontal areas. G–H) Follow-up MRI T2-weighted images 62 days later.